Transactions of Karelian Research Centre of
Russian Academy of Sciences
No. 3. 2017. P. 79–92
DOI: 10.17076/lim473

Труды Карельского научного центра РАН
№ 3. 2017. С. 79–92

МЕТОДЫ ИССЛЕДОВАНИЙ

УДК 551.482.213+528.8.04

BIO-OPTICAL RETRIEVAL ALGORITHM FOR THE OPTICALLY SHALLOW WATERS OF LAKE MICHIGAN. I. MODEL DESCRIPTION AND SENSITIVITY/ROBUSTNESS ASSESSMENT

A. A. Korosov[1], D. V. Pozdnyakov[1,2], R. Shuchman[3], M. Sayers[3], R. Sawtell[3], A. V. Moiseev[2]

[1] Nansen Environmental and Remote Sensing Center, Norway
[2] Scientific foundation "Nansen International Environmental and Remote Sensing Centre", Russia
[3] Michigan Tech Research Institute, USA

Lake Michigan (LM) is generally an oligotrophic clear water body, especially in its littoral zone where ecology-relevant processes unfold due to a variety of natural and anthropogenic forcings arising from the watershed. However, the bottom influence there is strong enough to contaminate the at-satellite signal, thus impeding the remote sensing of water quality parameters within the coastal zone. A new bio-optical retrieval algorithm, based on a forward radiation transfer model, LM specific hydro-optical model and the multivariate optimization technique are developed for operational retrieval from satellite data of water quality parameters in lake's optically shallow areas. As a result, the concentrations of major Color Producing Agents (CPAs), viz. phytoplankton chlorophyll, total suspended matter and yellow substance could be retrieved in transparent coastal waters with a variety of bottom cover types: sand, silt, stands of *Chara*, and *Cladophora*, and limestone pebble. The sensitivity of both forward and inverse models was tested for LM hydro-optical conditions. By means of forward simulations it is shown that at very low concentrations of CPAs (less than 0.01 in respective units) the optical influence of the bottom becomes indiscernible if the bottom depth, H approaches 20 m. In waters loaded with higher quantities of total suspended matter (TSM) and phytoplankton chlorophyll, CHL, the bottom influence ceases at H ~ 10 m. The noise sensitivity has shown that the shallower the water column and higher bottom albedo the more significant is the ensuing error in CPA retrievals. E. g. for a sandy bottom and water column of 5 m, a 10 % error in determining of albedo leads to a 18 %, 28 % and 10 % error in retrieving, respectively, CHL, TSM and colored dissolved organic matter, CDOM.

K e y w o r d s: optical remote sensing; spectral reflectance; attenuation; surface albedo; optically shallow waters; limnology; Lake Michigan.

А. А. Коросов, Д. В. Поздняков, Р. Шухман, М. Сайерс, Р. Соутелл, А. В. Моисеев. БИООПТИЧЕСКИЙ АЛГОРИТМ ВОССТАНОВЛЕНИЯ ПАРАМЕТРОВ КАЧЕСТВА ВОДЫ ДЛЯ ОПТИЧЕСКИ МЕЛКИХ ВОД ОЗЕРА МИЧИГАН. I. ОПИСАНИЕ МОДЕЛИ И ОЦЕНКА ЕЕ ТОЧНОСТИ/ НАДЕЖНОСТИ

Озеро Мичиган относится к олиготрофному типу водоемов. Сильнее всего это проявляется в прибрежной зоне, где гидрологический режим вод формируется под действием различных природных и антропогенных факторов, протекающих на водосборной территории. Влияние дна достаточно сильно искажает регистрируемый спутником сигнал, препятствуя выполнению дистанционного зондирования параметров качества воды в этой части озера. Для извлечения из спутниковых снимков параметров качества воды в оптически мелких районах озера Мичиган был разработан новый биооптический алгоритм. Он основан на модели переноса излучения, гидрооптической модели озера Мичиган и многомерной оптимизации и позволяет получать оценку концентрации всех основных оптически активных веществ (ОАВ) в областях с различным типом дна: песок, ил, макрофиты (*Chara* или *Cladophora*) и известняковая галька. Тестирование алгоритма показало, что при очень низких концентрациях ОАВ (менее 0,01 в соответствующих единицах измерения) оптическое влияние дна становится незначительным при глубине около 20 метров. В воде с более высокими концентрациями взвешенного вещества (ВВ) и хлорофилла влияние дна становится неразличимым при глубине ~10 м. Тестирование чувствительности алгоритма к шуму показало, что чем меньше толщина исследуемого водного столба и чем выше альбедо дна, тем выше погрешность восстановления концентраций ОАВ. Например, в случае песчаного дна и глубины 5 м погрешность в 10 % при оценке альбедо дна приводит к ошибкам в 18, 28 и 10 % при восстановлении хлорофилла, ВВ и окрашенного растворенного органического вещества соответственно.

Ключевые слова: дистанционное зондирование; спектральное отражение; альбедо дна; оптически мелкие воды; лимнология; озеро Мичиган.

Introduction

In the case of Lake Michigan, remote sensing encounters a serious methodological problem. With the exception of some bays and specific areas within the coastal zone, this Great Lake is an oligotrophic water body with optically clear waters [Effler et al., 2013]. Due to high water clarity, the bottom influence exerted on the light coming out from beneath the water surface is strong enough to contaminate the at-satellite signal [Gordon, Brown, 1974]. This is bound to impede the remote sensing of bulk water quality parameters within the coastal zone. The above problem is encountered in satellite studies of other littoral areas in the other four Laurentian Great lakes as well as many aquatic environments throughout the world's oceans. A variety of methodological approaches have been exploited to meet this challenge as described below.

The inverse problem solution (IPS) in the case of optically shallow waters consists in untangling the light signals originating from water column backscattering and bottom reflection. It offers a very important potential to retrieve the state and dynamics of both bottom topography [Hu, 2008], and bottom cover type [e. g. Hu et al., 2003; Dekker et al., 2011] due to river- and land-runoff [Hu et al., 2004, 2005], and climate change [Shuchman et al., 2006].

The distribution of seagrass and macrophytes across the bottom reflects the trophic state and quality of nearshore waters. At the same time, it is controlled by attenuation of sun light propagating through the water column due to water Color Producing Agents (CPAs) such as phytoplankton, dissolved organics, and tripton. In many applications, those two aspects of the IPS develop into either separate or combined tasks of remote sensing of optically shallow water bodies depending on the specific aims of surveillance.

The history of investigation of potentials of ocean color data to determine bottom depth and benthic cover types as well water constituents over large optically shallow areas exceeds several decades. Starting from predominantly empirical approaches [Lyzenga, 1978; Clark et al., 1987; Philpot, 1989], IPS methods have gradually developed into a specialized area of research.

In this study of Lake Michigan's peripheral zone, we develop a multiband **B**io-**O**ptical **RE**trieval **AL**gor**I**thm for **O**ptically **S**hallow **W**aters coined BOREALI-OSW. The algorithm retrieves CPA concentrations from remote sensing reflectance in clear

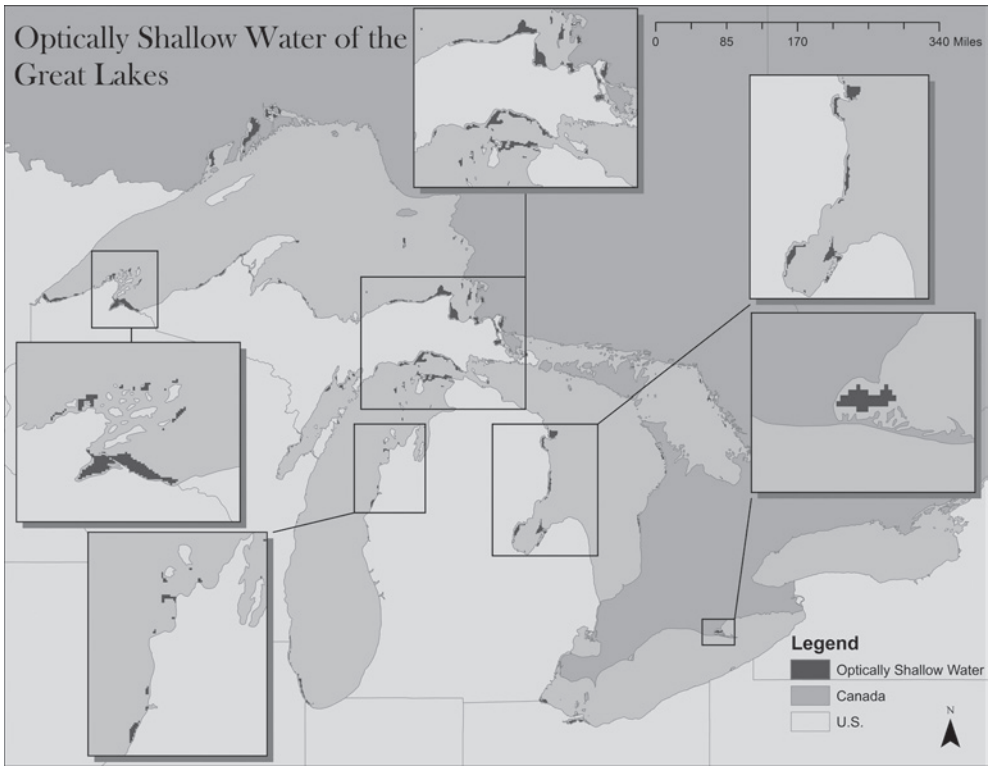

Fig. 1. Optically shallow water of the Great Laurentian Lakes

waters for a variety of bottom depths and bottom types. It is an extension of the BOREALI algorithm that has been previously developed for optically deep and turbid waters, went through thorough verification campaigns [Korosov et al., 2009] and proved its efficiency for a wide variety of water bodies including the North European and North American Great Lakes, among the latter – Lake Michigan [Shuchman et al., 2006].

Importantly, the BOREALI algorithm permits simultaneous retrieval of the concentrations of three ecologically important water quality constituents, viz. phytoplankton chlorophyll, suspended *minerals* and *dissolved organic matter*. The ability of the BOREALI algorithm to differentially provide quantitative information on these three water constituents makes its use particularly valuable for limnologists and water management agencies in their studies of ecological status and its dynamics driven by anthropogenic, invasive species and climatic forcing.

Due to the legacy of the BOREALI algorithm, the BORREALI-OSW algorithm also permits to simultaneously retrieve, in addition to phytoplankton chlorophyll content, the concentrations of suspended minerals and dissolved organic matter as opposed to those algorithms that retrieve just total suspended matter, or non organic suspended matter and absorption of colored dissolved organic matter [e. g. Dekker et al., 2011]. This distinction is very important for identification of the nature and intensity of inputs of substances into the coastal zone with the river- and land- runoff in order to get a better insight into the mechanisms of the ecosystem forcing. It is also valuable for ecological simulations as the models do not operate with total suspended composition or absorption of yellow substance, but with specific water quality constituents.

The distinguishing features of the BOREALI and BOREALI-OSW algorithms are, first and foremost, that they (i) require a manageable number of input parameters, (ii) are extendable to any aquatic environment, for which a dedicated hydro-optical model is available, (iii) do not require any preliminary tuning and are ready for use. BOREALI-OSW can also yield spectral values of $K_d(\lambda)$ in the water column over the bottom because it retrieves the concentrations of water color producing agents and uses the respective specific absorption and backscattering coefficients (see below eqs. 7 and 8, section 4). Finally, they are truly near-operational. The BOREALI-OSW algorithm employs the Levenberg-Marquardt multivariate optimization procedure, and uses in this study the recently established hydro-optical model of Lake Michigan [Shuchman et al., 2013a].

The BOREALI-OSW algorithm has the potential to be a very useful tool in studying littoral ecosystems throughout the entire Laurentian Great lakes. Figure 1 is a map of optically shallow water (red areas) in the five lakes where the use of

BOREALI-OSW is applicable. The majority of the areas mapped are areas of high concern from a resource management perspective.

This paper addresses the methodology of the elaborated tool, the assessment of its sensitivity to the hydro-optical conditions and types of substrates inherent in the coastal zone of Lake Michigan, as well as the accuracy of retrieval of the desired parameters. To test its performance, the algorithm is applied to simulated, field-measured and MODIS data. We show that its accuracy is superior to the standard OC4 algorithm [O'Reilly et al., 2000]. It can also be applied to other present and future multispectral spaceborne sensors such as NPP/VIIRS and Sentinel 3/OLCI.

Lake Michigan: a concise general description

Lake Michigan (41°35′N – 46°N; 85°W – 88°W, Fig. 2), like the four other Laurentian Great Lakes of North America, began to form at the end of the last glacial period approximately 10,000 years ago. Due to the nature of its formation (initially a pristine melt water body), morphometry (the average depth is 85 m, the water volume is 4,900 km^3 second largest by volume), thermal regime (even in summer, the water temperature at the bottom does not exceed 5 °C) and the watershed soil geochemistry [Gillespie et al., 2008] the lake was originally oligotrophic [Chapra et al., 1981].

It still remains mostly as such due to its glacial heritage, although there are indications that the lake's trophic status should now be defined as oligo-mesotrophic [Mida et al., 2010]. This is because Lake Michigan has been subjected to external pressure produced by climate warming (water temperature growth in upper layers), atmospheric fallouts (phosphorus deposition) and human activities (input of phosphorus and other pollutants, including toxic ones, through sewages and atmospheric deposition) as well as introduction of invasive species.

The anthropogenic impact proves to be especially pronounced in the southern part of Lake Michigan: there are the most urbanized areas in the

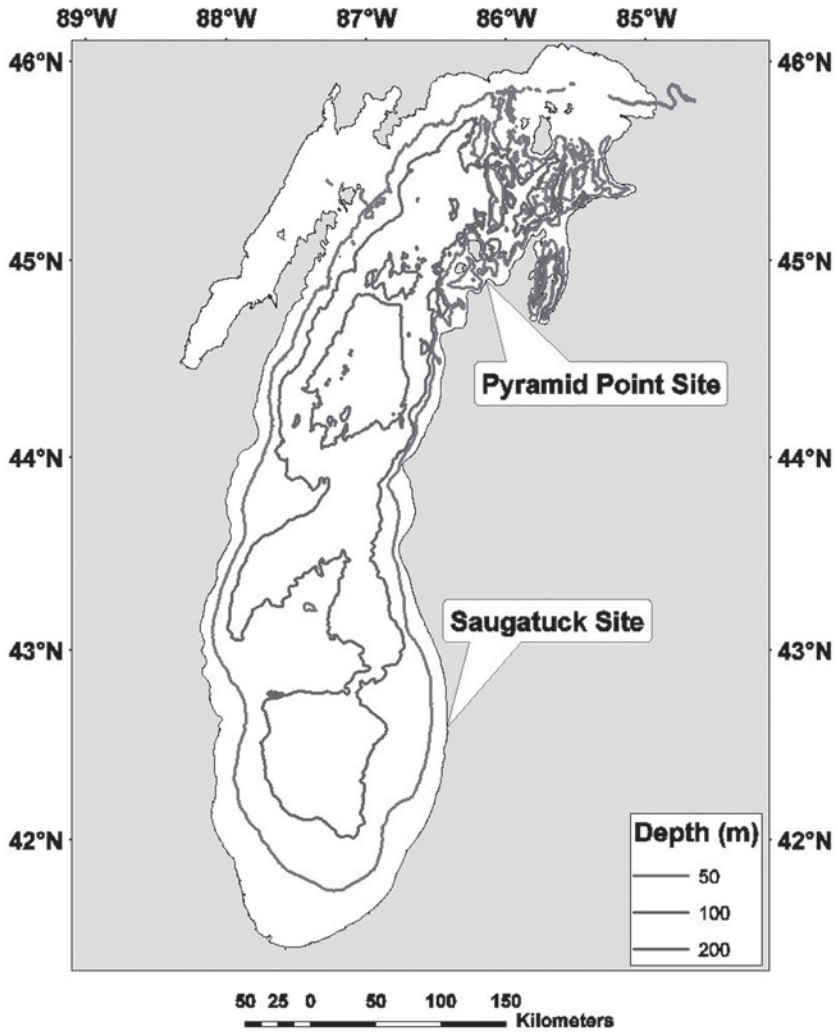

Fig. 2. Lake Michigan bathymetry

Table 1. Combinations of concentrations used in numerical experiments. Water type labels in the first column are referred to in the rest of the text

Water type label	C_{CHL}, mg m^{-3}	C_{TSM}, g m^{-3}	a_{CDOM}, m^{-1}
Clear water	0	0	0
CHL-dominated clear water	1	0	0
TSM-dominated clear water	0	0.2	0
Slightly turbid water	1	0.2	0.05
Turbid water	2	0.5	0.1
Very turbid water	5	1	0.5

Great Lakes system, whereas the northern part is less developed, sparsely populated with the exception of Green Bay, which is the recipient of waters of the Menominee River flowing through the Fox River Valley and carrying the wastes from the world's largest concentration of pulp and paper mills.

Some 186 invasive species have come to the Great Lakes, and among them are the quagga and zebra mussels entering the lakes in ballast water. Apart from damaging the lake ecosystem via disrupting some intrinsic trophic interactions, the mussels, as water filterers, increase the water transparency (e. g. at the Sleeping Bear Dunes the bottom visibility depth has increased from ca 2.5 m in 1970 up to 20 m in 2010) and thus let more solar light reach the bottom in shallow coastal zones [Nalera, Schloesser, 2014].

Phosphorous availability and mussels driven increased water clarity have resulted in the invigoration of benthic flora and macrophytes/submerged aquatic vegetation (SAV) as well as its proliferation to greater depths. (In Lake Michigan, *Cladophora* is the dominant SAV [Greb et al., 2004]).

Reportedly, the offshore extent of SAV generally does not exceed 5–10 m, although along the northernmost periphery of the lake the SAV standing stocks are found at depths nearing 20–25 m [Shuchman et al., 2013b].

Presently the phytoplankton community comprises four major groups: blue-green and green algae, diatoms and flagellates (http://www.glerl.noaa.gov/pubs/brochures/foodweb/LMfoodweb. pdf).

Methodology

Semi-empirical forward simulation

Hydro-optical model

The employed hydro-optical model is a set of the inherent optical properties (IOPs): spectral values of CPA specific (i. e., normalized to a respective CPA concentration) spectral coefficients of absorption, a^* and backscattering b^*_b of phytoplankton (CHL), and total suspended matter (TSM). The spectral influence of colored dissolved organic matter (CDOM) was confined in the model to its absorption measured in m^{-1}.

Due to the additive nature of IOPs, the bulk water inherent properties can be expressed as follows:

$$a(\lambda) = a_w + a^*_{CHL}C_{CHL} + a^*_{TSM}C_{TSM} + a^*_{CDOM}C_{CDOM} \quad (1)$$

$$b_b(\lambda) = b_{bw} + b^*_{bCHL}C_{CHL} + b^*_{bTSM}C_{TSM} \quad (2)$$

where w stands for water per se. In the present study, the hydro-optical model developed specifically for Lake Michigan was employed [Shuchman et al., 2013a].

Remote sensing reflectance

In our study we operate with the subsurface spectral remote sensing reflectance, R_{rsw}, which is the upwelling spectral radiance just below the water-air interface, $L(-0)$ normalized to the downwelling spectral irradiance, $E(-0)$ at the same level [e. g. Jerome et al., 1996]. The algorithm for computing R_{rsw} for optically shallow waters is based on the equation suggested by Maritorena et al. [1994] assuming that the coefficients of the upwelling and downwelling irradiance attenuation are equal and do not change with depth, H:

$$R(-0,H) = R_\infty + (A - R_\infty)\exp(-KH) \quad (3)$$

We can rewrite eq. 3 in the following form:

$$R(-0,H) = R_\infty[1-\exp(-2KH)] + A\exp(-2KH) \quad (4)$$

The diffuse and remote sensing reflectance above surface (R_{rs}) are interrelated through the following relationship [Bukata et al., 1995]:

$$R_{rs}(\lambda,+0) = R(\lambda,-0)/Q \quad (5)$$

where Q is the ratio of the upwelling irradiance below the water surface to the upwelling nadir radiance below the water surface. Hence, eq. 4 can be converted into the equation for total remote sensing reflectance R_{rsTOT} by dividing both parts of the equation by Q:

$$R_{rsTOT}(\lambda,+0) = R_{rsDEEP}[1-\exp(-2KH)] + \\ + A\exp(-2KH)/Q \quad (6)$$

where R_{rsDEEP} is the remote sensing reflectance of optically deep waters, K is the light attenuation coefficient, A is the bottom albedo and H is the depth. The value of K can be calculated using the Kirk [1984] parameterization:

$$K = (1/\mu_1)[a^2 + ab(0.473\mu_1 - 0.218)]^{1/2} \quad (7)$$

where μ_1 is the cosine of the solar zenith angle after refraction at the air-water interface, a is the

total absorption (eq. 1) and b is the total scattering [Bukata et al., 1995]:

$$b = \frac{b_{bw}}{0.5} + b_{bCHL} + \frac{C_{CHL}}{0.011} + \frac{b_{bTSM} C_{TSM}}{0.08} \qquad (8)$$

Remote sensing reflectance for deep waters is computed from the subsurface remote sensing reflectance (R_{rsw}) using semi-analytical formula suggested by Lee et al. [2002]:

$$R_{rsDEEP}(\lambda,+0) = \frac{0.5 R_{rsw}}{R_{rsw} - 1.7} \qquad (9)$$

where R_{rsw} is calculated using the parameterization suggested by Albert and Gege [2006] for a wide range of summer time sun elevation angles:

$$R_{rsw}(\lambda,-0) = 0.512G \cdot$$
$$\cdot(1 + 4{,}6659G - 7.8387G^2 + 5.4571G^3) \cdot \qquad (10)$$
$$\cdot(1 + 0.1098/\mu_1)(1 + 0.4021/\mu_2)$$

where $G = b_b / (b_b + a)$ and μ_2 is the cosine of the viewing nadir angle just below the surface. Ultimately, total subsurface remote sensing reflectance (R_{rswTOT}) is calculated from total remote sensing reflectance (R_{rsTOT}) using inversed eq. 9 [Lee et al., 2002]. The Q factor (eq. 6) value may vary in a wide range from π to 6 or even higher depending on water turbidity, sun zenith angle and viewing angle [Jerome, 1996; Mobley, 2002]. Based on the shipborne measurements conducted in Lake Michigan [EEGLE, 2003] we assume that for sun zenith angles below 30° (typical of summer-time illumination conditions within the Lake Michigan latitudinal belt) the Q factor does not vary significantly and on average is close to 4.

Inverse problem solution

The Levenberg-Marquardt algorithm

The problem of determination of the CPA concentration vector, C is solved using the multivariate optimization approach. The spectral difference between the measured (R_{rswM}) and reconstructed remote sensing reflectance (using eq. 10) (R_{rswTOT}) is calculated as:

$$g(C) = R_{rswM} - R_{rswTOT}(C) \qquad (11)$$

The absolute minimum of g is found with the Levenberg-Marquardt finite difference algorithm [Press et al., 1992], which assures a rapid convergence of the iterative procedure. The following iterative expression is used to this goal:

$$C_{k+1} = C_k (F_k^T F_k + \mu_k D_k)^{-1} F_k^T g \qquad (12)$$

where k is the iteration step, F is the Jacobian matrix, μ_k is the length and direction of minimization step, $D_k = diag\ (F_k^T F_k)$ is the diagonal of matrix of $F_k^T F_k$. The Jacobian matrix has n x m elements and is calculated as follows:

$$f_{i,j} = \partial g(\lambda_i, C_j) / \partial C_j \qquad (13)$$

where λ_i is the wavelength, at which R_{rsw} has been determined (i. e., i = 1–6 in case of MODIS with 6 spectral channels in the visible region), C_j is the CPA concentration (encompassed by the concentration vector C). In our simulations j = 1–3, i. e. only three components were considered, viz. C_{CHL}, C_{TSM} and a_{CDOM}. Thus, through a multivariate iterative procedure testing sequentially the values of CPA specific concentrations, the magnitude of the concentration vector C, for which the Jacobian matrix is the minimum, eventually defines the solution of the inverse problem.

Realization of the algorithm in the code

The algorithm is realized as a Python and C++ software package called Bio-Optical REtrieval AlgorIthm for Shallow waters [BOREALI-OSW, https://github.com/nansencenter/boreali]. The Python part consists of one class called Boreali and incorporates the procedures for opening input files, loading the values of specific absorption and backscattering coefficients from the text files and running the processing in several parallel threads. The C++ part consists of a hierarchy of classes called Hydrooptics and HydroopticsShallow and several interface functions that communicate with Python and CMINPACK library. The class Hydrooptics is designed for performing all hydro-optical calculations in deep waters and has separate procedures implementing eqs. 1, 2, and 10. The class HydroopticsAlbedo inherits from HydroopticsShallow and overrides methods implementing eqs. 6–9. The analytic formulas for calculating the elements of Jacobian matrices (presented in a general form in eq. 13) were excessively long and the discrete finite difference derivatives are used, which require less computations. The CMINPACK library was used for performing the Levenberg-Marquardt optimization procedure [More, 1984].

Numerical experiments with the forward model and BOREALI-OSW algorithm

Sensitivity analysis of the forward model

Several numerical experiments were conducted to test the applicability of the algorithm to processing of data from the Laurentian Great Lakes. In the first group of experiments, we tested the sensitivity of the forward model to variations in bottom depth and type as well as CPA concentrations. The spectral values of R_{rswTOT}

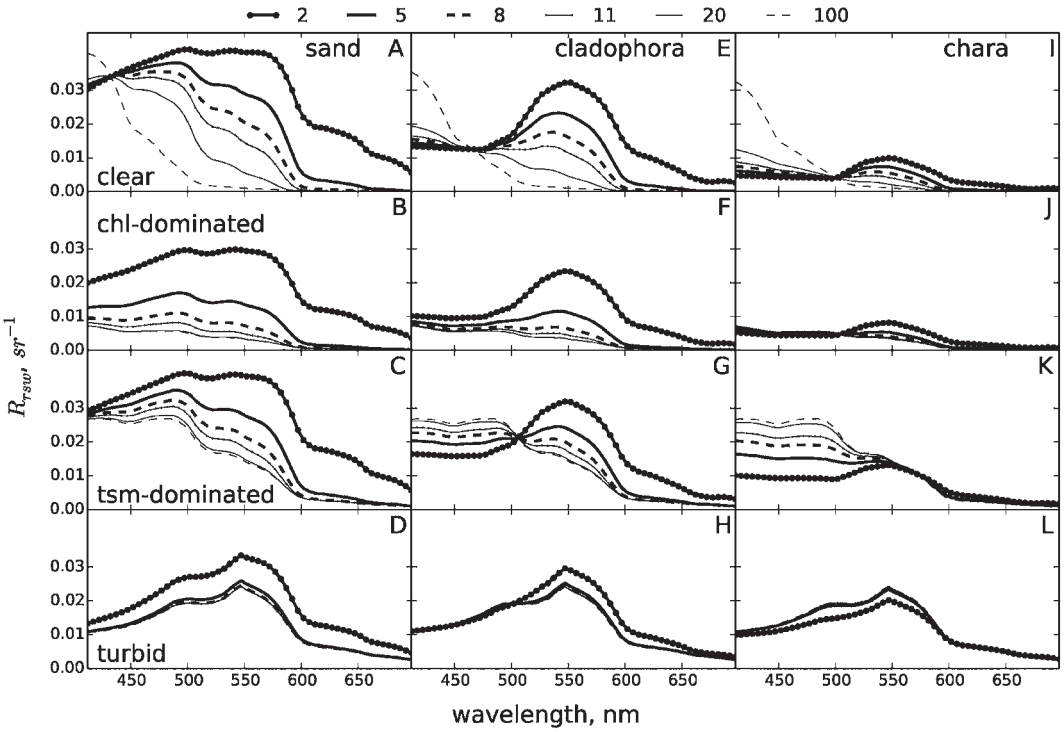

Fig. 3. Spectral values of R_{rswTOT} simulated for various combinations of 6 depths (denoted by the line style and thickness), 3 bottom types (in columns) and 4 combinations of CPA concentrations (in rows). The bottom type and the nicknamed water type are specified, respectively, in A, E, I and A – D boxes

were simulated for the following combinations of parameters typical of the Laurentian Great Lakes:

1. CPA concentration combinations are listed in Table 1;
2. Depths: 2, 5, 8, 11, 20, 100 m;
3. Bottom types: sand, silt, green algae *Chara sp.*, green algae *Cladophora glomerata*, and limestone pebble.

R_{rswTOT} spectra were plotted for each option specified above to reveal the responsiveness of R_{rswTOT} values to the variability in CPA concentrations and bottom depth and type. In addition, we studied the dependence of the spectrally averaged relative difference ($D_R = (R_{rswTOT} - R_{rswDEEP}) / R_{rswDEEP}$) on the same variables. The numerical simulations explicitly indicate (a few cases are exemplified in Fig. 3) that the bottom optical impact on R_{rswTOT} depends on a complicated interplay of all three factors: depth, bottom type and CPAs combinations. The strongest impact is observed in clear waters (the upper row of boxes in Fig. 3) but its intensity decreases as the concentration of one or several CPAs, i. e. CHL, TSM or CDOM, increases (the lower rows of boxes in Fig. 3).

In turbid waters, the impact is the lowest: only at a 2 m depth we can observe D_R of about 30 % whereas at more significant depths the bottom optical influence becomes undetectable. The sandy bottom (having the highest albedo averaged throughout the visible spectrum) exhibits the highest impact on the water leaving signal (the left column of plots in Fig. 3): D_R reaches 3600 % for a 2 m depth in clear waters. The bottom covered with *Cladophora* produces a significantly lower impact: $D_{R,2m}$ = 1400 % (the middle column in Fig. 3). Finally, a *Chara* – covered bottom (the third column in Fig. 3) and a silted bottom (not exemplified in Fig. 3) produce the lowest impact: $D_{R,2m}$ = 300 %.

The bottom optical impact may result in either a general increase in R_{rswTOT} (see e. g. the case of a sandy bottom in CHL- and TSM-dominated waters, Fig. 3, boxes B, F, G), or a general decrease of R_{rswTOT} (see e. g. the case of a *Chara*-covered bottom in TSM-dominated waters, Fig. 3, box K), or a decrease in the blue accompanied by an increase in the red (see e. g. the case of a *Cladophora*-covered bottom in TSM-dominated waters, Fig. 5, boxes A, E, G) as the bottom depth declines. If the bottom albedo is high enough, higher values of R_{rswTOT} are observed in shallow waters as opposed to deep waters: more sun light is reflected due to both reflectance from bottom and backscattering within the water column. Contrarily, in shallow waters at low values of albedo, the bottom reflects less light than that backscattered by the water medium, and the resultant R_{rswTOT} (see eq. 10) becomes lower as compared to that in deep waters.

Table 2. Depths (m) at which the reflection from the bottom significantly impacts the water leaving light signal (D_R > 10 %)

Bottom Type	Clear Water	CHL–Dominated	TSM–Dominated	Slightly Turbid	Very Turbid
Sand	60	15	11	7	3
Silt	50	12	4	5	2
Limestone	50	12	4	5	2
Cladophora	35	12	4	5	2

The spectral signature of R_{rswTOT} is conjointly controlled by the spectral features of absorption and backscattering of water per se and co-existing CPAs as well as the spectral curvature of bottom albedo. Thus, in the case of clear waters and a sandy/highly reflective bottom (whose albedo grows linearly with the wavelength, Fig. 4) the hyperbola like spectrum of pure water reflection enhances rapidly in the blue with decreasing bottom depth, and at 2 m depth the R_{rswTOT} spectrum acquires a dome-like shape with a broad flat top stretching from 500 to 600 nm (Fig. 3, box A). Even though the sand albedo is highest in the red (Fig. 4), the growth of R_{rswTOT} with decreasing bottom depth in this spectral region is subdued due to strong water absorption at wavelengths > 620 nm. For the *Cladophora*-covered bottom, whose spectral albedo is dome-like (Fig. 4), at 2 m depth a well-pronounced peak centered at 550 nm stands out as a salient spectral feature in R_{rswTOT} accompanied by a decrease in the blue and red parts of the spectrum.

A comparison of R_{rswTOT} in the case of CHL- and TSM-dominated waters (Fig. 3, boxes B, C), reveals, firstly, that at bottom depths exceeding 2 m, it is nearly twice higher for CHL-dominated waters. Secondly, increasing bottom depth in CHL-dominated waters leads to a higher absorption in the blue due to chlorophyll with a result of a significant reduction of R_{rswTOT} at λ = 400 nm (from 0.02 sr^{-1} at 2 m to 0.007 sr^{-1}) at 20 m, Fig. 3, box B.

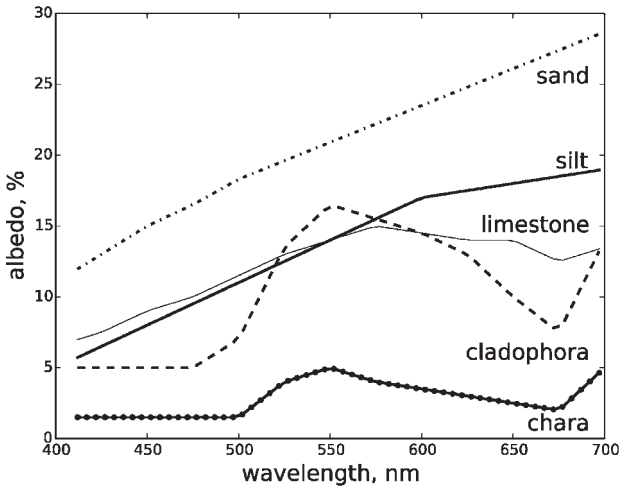

Fig. 4. Spectral values of bottom albedo used in our study (data from [Kutser et al., 2006])

Contrarily, in TSM-dominated waters, backscattering is the major player, and R_{rswTOT} at 400 nm remains almost intact with increasing bottom depth and retains a fairly high value (0.03 sr^{-1} Fig. 3, box C). In addition, due to backscattering by TSM the values of R_{rswTOT} are also enhanced in the red (ranging from 0.01 sr^{-1} at 2 m to 0.002 sr^{-1} at 5 m and deeper, Fig. 3, box C). This is in contrast with infinitesimal values of R_{rswTOT} for CHL-dominated waters when the bottom depth is in excess of 5 m (Fig. 3, box B).

At low bottom depths, R_{rswTOT} spectra in the case of CHL-dominated waters with a sandy bottom resemble rather closely R_{rswTOT} spectra originating from deep TSM-dominated waters: similar reflection enhancements at 490 and 550 nm, R_{rswTOT} values ranging from 0.03 to 0.005 sr^{-1} (Fig. 3, boxes B and C). It is the strong absorption of CHL-a and intense scattering by TSM which permit to unmistakably ascribe R_{rswTOT} spectra to waters categorized as CHL- and TSM dominated: spectra from shallow CHL-dominated waters should have lower values in the blue and red comparing to spectra from deep TSM-dominated waters.

The value of D_R decreases with the increase of either bottom depth or CPA concentrations, and this decrease depends on the bottom type. When D_R reaches some critical value, e. g. 10 %, it is an indication that the uncertainty in measurements of R_{rswTOT} is higher than the method's sensitivity to the bottom optical influence. Table 2 illustrates our estimations of the depth, at which D_R is above 10 % under different in-water conditions, i. e. combinations of CPA values and bottom types. At higher values of bottom depths, the correction for the bottom optical impact is not worth applying.

Our simulations indicate that in ideally clear waters even a *Chara*-covered bottom may be seen at depths of 11 meters, while sandy bottoms are discernible at depths of 60 meters. However, the presence in the water column of even low amounts of CHL or TSM reduces these depths to, respectively 4 and 15 meters. In turbid waters, the depth at which we can potentially detect the bottom optical impact is 3–7 meters and it is only 2 m or even less in very turbid waters.

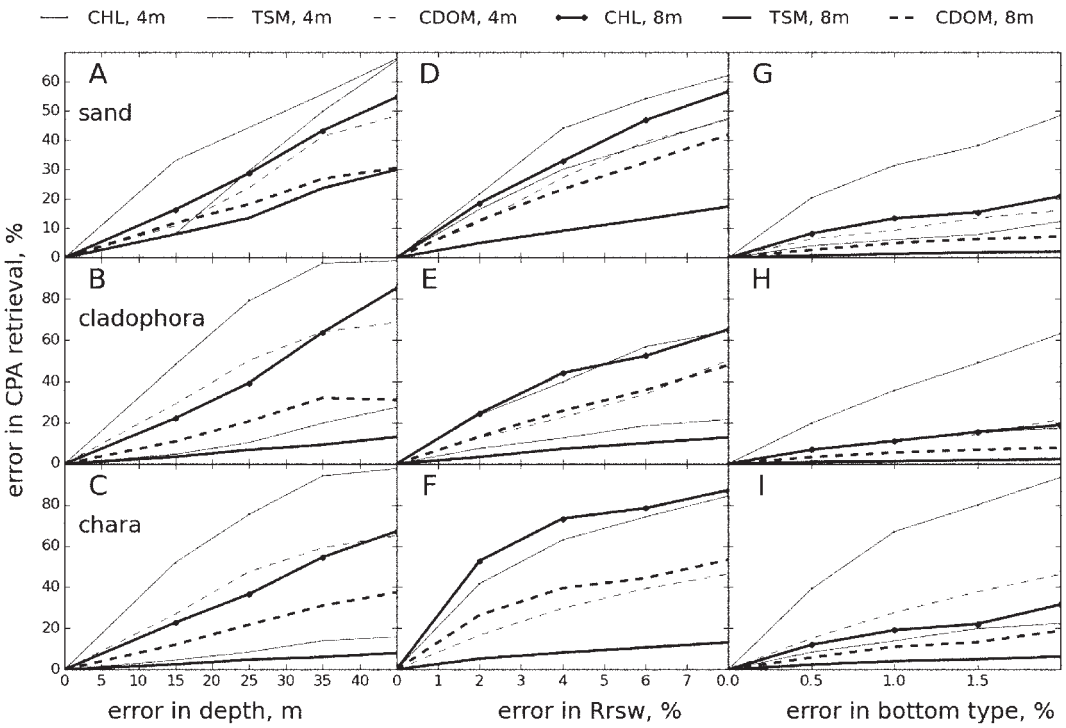

Fig. 5. Relative error of CPA concentration retrievals under various in-water conditions. Results of the numerical experiments are presented in three rows of boxes for each bottom type (sand, *Chara*-covered, *Cladophora*-covered) and three columns of boxes for each variable (depth, R_{rswTOT}, albedo). Each box contains plots for CHL (dotted line), TSM (solid line) and a_{CDOM} (dashed line) for two depths: 4 m (thin lines) and 8 m (thick lines). Results for a silt-covered bottom are not illustrated as they are very similar to those pertaining to the *Chara*-covered bottom

Thus summing up, the performed numerical simulations show that our model provides quite realistic values of R_{rswTOT} and accurately accounts for the various factors that affect its spectral shape. It is revealed that R_{rswTOT} spectra may be similar regardless of different water composition and bottom depth conditions (e. g. CHL-dominated shallow-waters or TSM-dominated deep waters). At the same time it is shown that there are features that make the reflectance spectra attributable to specific types of hydro-optical situations. Our analysis of D_R values permitted to identify conditions when the correction for bottom influence is mandatory.

Numerical experiments with the inverse problem solution.

Sensitivity of the retrieval algorithm to noise in input data

Sensitivity of the BOREAL-OSW algorithm is defined as a dependence of the error in retrievals of CPA concentrations on the errors in input values of either depth, H or reflectance, R_{rsw} or bottom type albedo, A. The sensitivity was estimated through numerical experiments involving the following three steps: (i) simulation of spectral R_{rswTOT} values using the afo-respecified parameterizations suggested by Kirk [1984], Bukata et al. [1995], and Albert and Gege [2006] for K_d [Pozdnyakov, Grassl, 2003], b [Bukata et al., 1995] and R_{rsw}, respectively for a given set of CPA concentrations, water depths and bottom types; (ii) contamination of either H, R_{rswTOT}, or A with different levels of noise; (iii) retrieval of CPA concentrations and comparison with the ones used in the first step simulations. For each experiment 1000 vectors of CPA concentrations were randomly generated within the following concentration ranges: CHL: 0–5 mg/m^3, TSM: 0–2 g/m^3, aCDOM: 0–0.5 m^{-1}.

The experiments were performed for three bottom types: sandy bottom, *Chara*-covered bottom and *Cladophora*-covered bottom, and for two depths: 4 and 8 m. Alterations of H were performed by adding a normally distributed noise with a standard deviation equal to 0, 0.5, 1, 1.5 and 2 m. Alterations of R_{rswTOT} were simulated by adding wavelength-independent normally distributed noise with a standard deviation equal to 0, 2, 4, 6 and 10 %. Alterations of spectral bottom albedo, A were enforced through spectral mixing of the correct A values with a 15, 25, 35 and 50 % departure. To compare simulated and retrieved CPA concentrations a normalized root mean square error ($\tilde{E}$) expressed in percent was employed:

$$\tilde{E} = 100\sqrt{\frac{\sum_j (C_{ij}^S - C_{ij}^R)^2}{nC_{ij}^S}} \qquad (14)$$

where C_{ij}^S is the simulated concentration of the i-th CPA in the j-th concentration vector, C_{ij}^R is the reconstructed CPA concentration, n is the number of vectors.

The results of our numerical experiments reveal (Fig. 5) that although the accuracy of CPA concentration retrieval exhibits a strong dependence on noise in input data, the algorithm remains reasonably robust.

Unlike deep waters, in shallow waters, the BOREALI-OSW algorithm is very sensitive to errors in the bottom depth, H (Fig. 5, boxes A, B, C). If the bottom has a high value of albedo (e. g. covered by sand), underestimation of depth even by 0.5 m results in misinterpretation of high spectral values of R_{rswTOT}, which are attributed to high values of TSM, thus increasing $\tilde{E}_{TSM}$ to 30 %. In the case of a darker bottom (e. g. *Chara*-covered), errors in TSM retrievals do not exceed 15 % even in shallow waters and the data on depth noised up to 2 m (Fig. 5, boxes B, C). The results of retrieval of CHL and a_{CDOM} are more sensitive to noise in depth and $\tilde{E}$ may exceed 20 % if the noise in depth is as low as 0.5 m.

The BOREALI-OSW algorithm proves to be very sensitive to errors in R_{rsw} with the worst results obtained for CHL ($\tilde{E}_{CHL}$ exceed 20 % if only a 2 % noise is added to R_{rsw}). However, it performs with this noise much better for TSM ($\tilde{E}_{TSM}$ does not exceed 20 % even if noise in R_{rsw} reaches 8 % at any depth or for any bottom type) (Fig. 5, boxes D, E, F). The algorithm is especially sensitive to noise in R_{rsw} for the *Chara*-covered bottom (Fig. 5, box F), i. e. when the bottom albedo is low.

In shallow waters, the error in bottom type mainly affects the accuracy of CHL retrieval: $\tilde{E}_{CHL}$ rises above 20 % already at a 15 % error in bottom type (Fig. 5, boxes H, I, J). In deep waters the value of $\tilde{E}$ for TSM and CDOM does not exceed 20 % even if the error in bottom type is as high as 50 %.

Table 3 summarizes the results of the BOREALI-OSW algorithm sensitivity experiments and specifies the conditions when the algorithm can be applied with acceptable accuracy (i. e., the average $\tilde{E}$ for all three CPAs is below 30 %). The conditions listed in Table 3 are quite realistic and can be encountered in a variety of natural water bodies. This fully justifies the application of BOREALI-OSW in the Laurentian Great Lakes.

Table 3. Maximum levels of noise in H, R_{rswTOT}, and A resulting in averaged values of $\tilde{E} < 30$ %. The first and second numbers stand for a 4 m and 8 m depth, respectively

Altered Variable	Sand	Cladophora	Chara
H	0.5 m, 1 m	0.5 m, 1.5 m	0.5 m, 3 m
R_{rswTOT}	3 %, 6 %	6 %, 10 %	2 %, 3 %
A	50 %, 80 %	50 %, 90 %	35 %, 95 %

Discussion

In the following discussion we are focusing on two key aspects of the results intended to meet the original objectives set up in the present study: development of a bio-optical retrieval algorithm for very clear / optically shallow waters, and assessment of its potentials as an operative tool for satellite-based monitoring of the coastal zone of Lake Michigan.

Correspondingly, such an algorithm, named BOREALI-OSW, and the respective code were elaborated. The BOREALI-OSW algorithm is based on the Levenberg-Marquardt multivariate optimization technique, a hydro-optical model established specifically for Lake Michigan, and a few parameterizations relating (i) the bulk water column inherent optical properties (absorption and scattering) to the CPA concentration vector, C and (ii) the subsurface remote sensing reflectance to C, bottom type and depth as well as the sun illumination conditions.

Quite expectedly, the simulations revealed that the optical influence of the bottom reflection becomes progressively less pronounced with increasing C and absorption capacity of the substrate. However, possibly due to the CPA properties inherent in Lake Michigan, this dependency proves to be very steep: even in relatively clear water conditions (often found in many lacustrine aquatic environments: C_{CHL} = 1 mg/m^3, C_{TSM} = 0.2 g/m^3, a_{CDOM} = 0.05 m^{-1}), the most reflective (sandy) bottom does not impact appreciably the upwelling signal starting with H = 7 m, and it is optically inconsequential at H = 3–5 m, if the substrate is either *Cladophora* or *Chara*. In waters labeled by us as very turbid (C_{CHL} = 5 mg/m^3, C_{TSM} = 1.0 g/m^3, a_{CDOM} = 0.5 m^{-1}) (in reality, it is a rather conditional ascription because in many inland and shelf sea waters within the temporal latitudinal zone such waters should rather be subsumed under the category of relatively clear waters [Pozdnyakov, Grassl, 2003]), the water leaving signal is already immune to the optical impact of bottom, whose depth is about 2 m.

Our numerical simulations have shown that for the water type gradation adopted, TSM-dominated waters unlike CHL-dominated waters obscure the bottom far more radically: with the exception of a sandy bottom case, a bottom depth of 4 m is already a limit for affecting the CPA retrieval results.

It is worth mentioning that depending on the bottom depth and substrate type as well as the water composition, the spectra of total subsurface remote sensing reflectance, R_{rswTOT} might resemble

each other, e. g. in the case of CHL-dominated waters with a sandy bottom they resemble rather closely R_{rswTOT} spectra originating from deep TSM-dominated waters. Our simulations are explicitly indicative that this resemblance is entirely due to the specific features of CHL and TSM inherent optical properties.

Interestingly, irrespective of the spectral signature of the bottom substrate considered in our study, the spectral distribution in R_{rswTOT} exhibits invariably a prevalent bell-like maximum (at about 550 nm). This maximum decreases with water turbidity and bottom reflectivity. It is also noteworthy that the maximum is centered spectrally differently, but this difference is rather slight for all water composition options and bottom types. However, for low reflective/vegetated bottoms the water column becomes more reflective at shorter wavelength, especially in the TSM-dominated as opposed to CHL-dominated cases.

Based on numerical simulations, the developed coded model has been further submitted to a thorough analysis to reveal its sensitivity to the accuracy of such input parameters as bottom depth, *H* and bottom albedo/bottom type.

The retrievals of TSM with the BOREALI-OSW algorithm are vulnerable to errors in the bottom depth, *H* provided the substrate albedo is high. Contrarily, the retrievals of CHL and aCDOM suffer from errors in *H* estimations in the case of vegetated substrates: NRSMSE may exceed 20 % if the noise in depth is even below 0.5 m. Understandably, these effects arise completely from the spectral features of absorption and backscattering of respective CPAs: it is suffice to remind that CHL and CDOM are optically most active in the blue whereas TSM transforms the upwelling light predominantly at the wavelengths in excess of 550 nm.

The BOREALI-OSW performance efficiency is also susceptible to errors in R_{rswTOT}. This is particularly so for the retrievals of CHL and significantly less for restoring TSM. The former is accentuated in the case of vegetated substrates, and low bottom depths. As Table 5 illustrates, depending on the bottom type, the permissible errors in R_{rswTOT} ($\tilde{E} <$ 30 %) must be within very narrow limits (2–6 %) at H = 4 m, which is a serious challenge given the typical inaccuracies in atmospheric correction inherent in level 2 data of MODIS [IOCCG, 2010]. The requirements to the accuracies in *A*, and, to certain degree, in *H* are less stringent and believed to be realistically attainable.

Assessing in general the performance of the developed code it can be defended that at least for bottom depths under ca 10 m the application of the BOREALI-OSW algorithm accounting for bottom optical influence yields CHL values appreciably closer to those determined in the laboratory as compared to CHL retrievals performed with the algorithms neglecting the bottom effect. At sites with a deeper bottom depth, the difference between the retrievals taking into account and neglecting the bottom optical impact progressively decreases, however it persists thus giving additional evidence in favor of the application of the BOREALI-OSW algorithm.

Conclusions

In attacking the problem of remote sensing of optically shallow waters with the purpose of retrieving concentrations of CPAs against the background of the light signal originating from bottom reflections, we pursued two avenues. Firstly, by means of forward simulations we analyzed through the spectral signature variations of subsurface remote sensing reflectance, R_{rsw} the modifications of the upwelling signal (controlled by the bottom type and depth). Then we passed to inverse problem simulations in order to test the sensitivity of our calculations of CPA concentrations to possible excursions of the input parameters such as bottom depth, bottom type, and measured spectral values of subsurface remote sensing reflectance, R_{rswTOT}. To do that, we developed a retrieval algorithm (BOREALI-OSW) dedicated specifically to cope with optically shallow waters.

To achieve the forward problem solution, we employed the hydro-optical model inherent in Lake Michigan water, and considered the bottom types encountered in this water body, viz. silicon sand, *Cladophora/Chara*, limestone rocks, and silt.

Our simulations have shown that even at very low CPA concentrations (less than 0.01 in respective units) the optical influence of the bottom becomes indiscernible, if the bottom depth, *H* approaches 20 m. In waters containing the total suspended matter (TSM) in quantities of about 0.5 g/m^3 (while CHL and colored dissolved organic matter, CDOM remain infinitesimal) the bottom optical influence ceases at *H* slightly above 10 m. An analogous critical value of *H* was found if a_{CDOM} is 0.5 m^{-3}, while CHL and TSM are infinitesimal.

The noise sensitivity analysis has shown that the shallower the water column and higher bottom albedo the more significant is the ensuing error in CPA retrievals. However, even in the case of a sandy bottom and a water column of 5 m, a 10 % error in determining its albedo leads to a 18 %, 28 % and 10 % error in retrieving, respectively, CHL, TSM and CDOM. In the case of deeper waters (H = 10 m) the noise in all considered CPA retrievals becomes lower than 4 %, 10 % and 4 % for CHL, TSM and CDOM, respectively.

Our analysis of the dependence of normalized root mean square error, $\tilde{E}$ in CPA concentration determinations on the noise level in input values of bottom depth, H and bottom albedo, A has shown that $\tilde{E}$ values can reach 18 %, ~30 % and 10 % for CHL, TSM and CDOM, respectively, if the noise in H is 10 %, but they become much higher (55 %, 55 % and 17 % for CHL, TSM and CDOM, respectively) if the noise in A is 10 %.

Our numerical assessment of the BOREALI-OSW algorithm performance in real conditions of Lake Michigan convincingly shows that at least for bottom depths less than 10 m its application to *in situ* radiometric data yields CHL values appreciably closer to those determined in the laboratory as compared to CHL retrievals performed with the algorithms neglecting the bottom effect. At sites with the deeper bottom depths, the difference between the retrievals taking into account and neglecting the bottom optical impact progressively decreases, however, remains appreciable thus giving additional evidence in favor of the application of the BOREALI-OSW algorithm.

This investigation was supported by NASA Roses Grant # NNX09AU88G and Michigan Tech Research Institute Internal Research and Development.

References

Albert A., and Gege P. Inversion of radiance and remote sensing reflectance in shallow water between 400 and 800 nm for calculations of water and bottom properties. *Applied Optics.* 2006. Vol. 45, no. 10. P. 2331–2343.

Bukata R., Jerome J., Kondratyev K., Pozdnyakov D. Optical Properties and Remote Sensing of Inland and Coastal Waters. Boca Raton: CRC Press, 1995. 362 p.

Chapra S. C., Dobson H. F. H. Quantification of the Lake Trophic Typologies of Naumann (Surface Quality) and Thienemann (Oxygen) with Special Reference to the Great Lakes. *International Association for Great Lakes Research*. 1981. Vol. 7, no. 2. P. 182–193.

Clark R., Fay T., Walker C. Bathymetry calculations with Landsat 4 TM imagery under a generalized ratio assumptions. *Applied Optics.* 1987. Vol. 26. P. 4036–4038. doi: 10.4319/lo2003.48.1 part^2.0431

Dekker A., Phinn S., Anstee J., Bissett P., Brando V., Casey B., Fearns P., Hedley J., Knlonowski W., Lee Z. P., Lynch M., Lyons M., Mobley C. Intercomparison of shallow water bathymetry, hydro-optics, and benthos mapping techniques in Australian and Caribbean coastal environments. *Limnology and Oceanography: Methods*. 2011. Vol. 9. P. 396–425.

EEGLE ship-collected data archive. 2003. 1, 2. CD-ROM.

Effler S., Peng F., O'Donnell D., Strait C. The backscattering coefficient and its components in the Great Lakes: A review and synthesis. *Journal of Great Lakes Research.* 2013. Vol. 39 (supplement 1). P. 108–122.

Gillespie R., Harrison III W. B., Grammer G. M. Geology of Michigan and the Great Lakes. *Western Michigan University Publ.* 2008. 37 p.

GITHUB: https://github.com/nansencenter/boreali (accessed: 20.08.2016).

Gordon H., Brown O. Influence of bottom depth and albedo on the diffuse reflectance of a flat homogeneous ocean. *Applied Optics.* 1974. Vol. 13, no. 9. P. 2153–2159.

Greb S., Garrison P., Pfeiffer S. Cladophora and water quality of Lake Michigan: a systematic survey of Wisconsin nearshore areas. In: Bootsma H. A., Jensen E. T., Young E. B., Berges J. A. (Eds.), Cladophora Research and Management in the Great Lakes. Special Report 200501. Great Lakes Water Institute, University of Wisconsin, Milwaukee. 2004. 7380 p.

Hu C. Ocean color reveals sand ridge morphology on the West Florida Shelf. IEEE *Geoscience and Remote Sensing Letters.* 2008. Vol. 5, no. 3. P. 443–447.

Hu C., Hackett K., Callahan M., Andrfout S., Wheaton J., Porter J., Mueller-Karge F. The 2002 ocean colour anomaly in the Florida Bight: A cause of local coral reef decline? *Geophysical Research Letters*. 2003. Vol. 30, no. 3. doi: 10.1029/2002GL016479

Hu C., Mueller-Karge F., Vargo G., Neely M., Johns E. Linkages between coastal runoff and the Florida Keys ecosystem: A study of a dark plume event. *Geophysical Research Letters.* 2004. Vol. 31. L15307. doi: 10.1029/2004GL020382

Hu C., Nelson J., Johns E., Chen Z., Weisberg R., Mueller-Karge F. Mississipi River water in the Florida Straits in the gulf Stream off Georgia in summer 2004. *Geophysical Research Letters.* 2005. Vol. 32. L14006. doi: 10.1029/2005GL022942

IOCCG. Atmospheric correction for remotely-sensed ocean colour products. Wang, M. (Ed.). Reports of the International Ocean-Colour Coordination Group. 10, IOCCG Publ. Dartmouth, Canada. 2010.

Jerome J. H., Bukat R. P., Miller J. R. Remote sensing reflectance and its relationship to optical properties of natural water. *International Journal of Remote Sensing*. 1996. Vol. 17, no. 1. P. 43–52.

Kirk J. T. O. Dependence of relationship between inherent and apparent optical properties of water on solar altitude. *Limnology and Oceanogaphy*. 1984. Vol. 29. P. 350–356.

Korosov A. A., Pozdnyakov D. V., Folkestad A., Pettersson L. H., Sörensen K., Shuchman R. Semi-empirical Algorithm for the Retrieval of Ecology-Relevant Water Constituents in Various Aquatic Environments. *Algorithms*. 2009. Vol. 2. P. 470–497.

Kutser T., Vahtmäe E., and Metsamaa L. Spectral library of macroalgae and benthic substrates in Estonian coastal waters. *Proc. Estonian Acad. Sci. Biol. Ecol.* 2006. 55 (4). P. 329–340.

Lee Z., Carder K., Arnone R. Deriving inherent optical proprerties from water color: a multiband quasi-analytical algorithm for optically deep waters. *Applied Optics.* 2002. Vol. 41, no. 27. P. 5755–5772.

Lyzenga D. Passive remote sensing techniques for mapping water depth and bottom features. *Applied Optics.* 1978. Vol. 17, no. 3. P. 379–383.

Mida J. L., Scavia D., Fahnenstiel G. L., Pothoven S. A., Vanderploeg H. A., Dolan D. M. Long-term and recent changes in southern Lake Michigan water quality with implications for present trophic status, *Journal of Great Lakes Research.* 2010. Vol. 36 (Supplement 3). P. 42–49. doi:10.1016/j.jglr.2010.03.010

Maritorena S., Morel A., Gentili B. Diffuse reflectance of oceanic shallow waters: Influence of water depth and bottom albedo. *Limnology and Oceanography.* 1994. Vol. 39, no. 7. P. 1689–1703.

Mobley C. D., Sundman L. K, Boss E. Phase Function Effects on Oceanic Light Fields. Applied Optics. 2002. Vol. 41, no. 6. P. 1035–1050. doi: 10.1364/AO.41.001035

More J. J., Sorensen D. C., Hillstrom K. E., Garbow B. S. The MINPACK Project, in Sources and Development of Mathematical Software, W. J. Cowell, ed., Prentice-Hall. 1984. P. 88–111.

Nalera T. F., Scholoesser D. W. (Eds.). Quagga and zebra mussels: biology, impacts and control. Boka Raton. CRC Press. 2014. 761 p.

O'Reilly J. E., Maritorena S., Siegel D., O'Brien M., Toole D., Mitchell B. G., Kahru M., Chavez F., Strutton P., Cota G., Hooker S., McClain C., Carder K., Muller-Karger F., Harding L., Magnuson A., Phinney D., Moore G., Aiken J., Arrigo K., Letelier R., Culver M. Ocean color chlorophyll a algorithms for SeaWiFS, OC2, and OC4: Version 4. In: O'Reilly, J. E., and 24 Coauthors. SeaWiFS Postlaunch Calibration and Validation Analyses, Part 3. NASA Tech. Memo. 11, S. B. Hooker and E. R. Firestone, Eds., NASA Goddard Space Flight Center, Greenbelt, Maryland. 2000. P. 9–23.

Philpot W. D. Bathymetric mapping with passive multispectral imagery. *Applied Optics.* 1989. Vol. 28, no. 8. P. 1569–1578.

Pozdnyakov D. V., Grassl H. Colour of Inland and Coastal Waters: a methodology for its interpretation. Chichester: Springer-Praxis, 2003. 170 p.

Press W., Teukolsky S., Vettering W., Flannery B. Numerical Recipes in C: The Art of Scientific Computing. 2nd ed. New York: Cambridge University Press, 1992.

Shuchman R. A., Leshkevich G., Sayers M. J., Johengen T. H., Brooks C. N., Pozdnyakov D. An algorithm to retrieve chlorophyll, dissolved organic carbon, and suspended minerals from Great Lakes satellite data. *Journal of Great Lakes Research.* 2013a. Vol. 32. P. 14–33.

Shuchman R. A., Sayers M. J., Brooks C. N. Mapping and monitoring the extent of submerged aquatic vegetation in the Laurentian Great Lakes with multi-scale satellite remote sensing. *Journal of Great Lakes Research*. 2013b. Vol. 39. P. 78–89.

Shuchman R., Korosov A., Hatt C., Pozdnyakov D., Means J., Meadows G. Verification and application of a bio-optical algorithm for Lake Michigan using SeaWIFS: a 7-year inter-annual analysis. *Journal of Great Lakes Research*. 2006. Vol. 32. P. 258–279.

Received August 22, 2016

СВЕДЕНИЯ ОБ АВТОРАХ:

Коросов Антон Андреевич
научный сотрудник, руководитель группы дистанционного зондирования морского и материкового льда, к. ф-м. н.
Центр по окружающей среде и дистанционному зондированию имени Нансена
Берген, Норвегия
эл. почта: anton.korosov@nersc.no

Поздняков Дмитрий Викторович
заместитель директора по науке,
руководитель группы водных экосистем,
д. ф.-м. н., проф.
Научный фонд «Международный центр по окружающей среде и дистанционному зондированию имени Нансена»
14-я линия В. О., 7, оф. 49, Санкт-Петербург,
Россия, 199034
эл. почта: dmitry.pozdnyakov@niersc.spb.ru

Шухман Роберт
директор, PhD
Мичиганский технический исследовательский институт
Анн-Арбор, США
эл. почта: shuchman@mtu.edu

Сайерс Михаэл
научный сотрудник
Мичиганский технический исследовательский институт
Анн-Арбор, США
эл. почта: mjsayers@mtu.edu

CONTRIBUTORS:

Korosov, Anton
Nansen Environmental and Remote Sensing Center
Thormøhlens gate, 47, N-5006, Bergen, Norway
e-mail: anton.korosov@nersc.no

Pozdnyakov, Dmitry
Scientific foundation "Nansen International Environmental and Remote Sensing Centre"
14th Line, 7, Office 49, Vasilievsky Island,
199034 St. Petersburg, Russia
e-mail: dmitry.pozdnyakov@niersc.spb.ru

Shuchman, Robert
Michigan Tech Research Institute
3600 Green Court, Suite 100, MI 48105, Ann Arbor, USA
e-mail: shuchman@mtu.edu

Sayers, Michael
Michigan Tech Research Institute
3600 Green Court, Suite 100, MI 48105, Ann Arbor, USA
e-mail: mjsayers@mtu.edu

Соутелл Реид
научный сотрудник
Мичиганский технический исследовательский институт
Анн-Арбор, США
эл. почта: rwsawtel@mtu.edu

Моисеев Артем Владимирович
младший научный сотрудник
Научный фонд «Международный центр по окружающей среде и дистанционному зондированию имени Нансена»
14-я линия В. О., 7, оф. 49, Санкт-Петербург, Россия, 199034
эл. почта: artem.moiseev@niersc.spb.ru

Sawtell, Reid
Michigan Tech Research Institute
3600 Green Court, Suite 100, MI 48105, Ann Arbor, USA
e-mail: rwsawtel@mtu.edu

Moiseev, Artem
Scientific foundation “Nansen International Environmental and Remote Sensing Centre”
14th Line, 7, Office 49, Vasilievsky Island,
199034 St. Petersburg, Russia
e-mail: artem.moiseev@niersc.spb.ru